Electronic Supporting Information

Synthesis, Structural Characterization and Biological Properties of Cyclometalated Iridium(III) Complexes Containing [1,2,5]-thiadiazolo-[3,4-f]-[1,10]-phenanthroline

Satish S. Bhat,[a] Naveen S.,[b,c] Vidyanand K. Revankar,[a] N. K. Lokhanath,[d] Rahul V. Pinjari,[e] Vijay Kumbar,[f] Kishore Bhat[f]

Methods and Instrumentation

The ^{1}H and ^{13}C NMR spectra of tdzp ligand dissolved in chloroform (d_1) and iridium complexes dissolved in DMSO (d_6) were recorded on a Jeol 400 MHz spectrometer at room temperature. The IR spectra of solid samples of iridium complexes **1** and **2** dispersed in KBr were recorded on a NICOLET, USA model-NICOLET 6700, FT/IR infrared spectrometer. Microanalysis (C, H, and N) of column purified complexes **1** and **2** were done with a Thermo Quest microanalysis instrument accomplished of carrying out C, H, N (carbon, hydrogen, nitrogen) analysis. The electrospray ionization mass spectra of **1** and **2** dissolved in chloroform were measured on waters UPLC-TQD triple quadrupole mass spectrometer. The Jasco V670 spectrophotometer was used to record all electronic spectra of complexes. The Hitachi F-7000 fluorimeter was used to record emission spectra. The high-resolution optical microscope, Axio Imager 2, Carl Zeiss, Germany was used to capture fluorescence microscopy images of cells.

Emission quantum yields (ϕ) were calculated by integrating the area under the fluorescence curves and by using equation 1[1]

$$\phi_{Sample} = \{OD_{Standard} \times A_{Sample}\}/\{OD_{Sample} \times A_{Standard}\} \times \phi_{Standard} \quad \text{---------- (1)}$$

Where OD is the optical density of the compound at the excitation wavelength (370 nm) and A is the area under the emission spectral curve. Relative quantum yields are compared to $[Ru(bpy)_3]^{2+}$ ϕ=0.028 in aerated aqueous solution [2]. The Quantum yield values are corrected for the refractive index of the solvent according to reference [3].

X-ray Crystallography

The single-crystal X-ray diffraction data for complex **1** and **2** were recorded at 173 K on a Bruker X8 Proteum diffractometer furnished with an X-ray producer operating at 45 kV and 10 mA, using Cu-Kα radiation (λ=1.54178 Å). The complete data sets were processed using SAINT PLUS [4]. The structure of complexes 1 and **2** were solved on Olex2 [5] using the SHELXT

program and refined (full-matrix least-squares refinement on F^2) using SHELXL program [6]. All non-hydrogen atoms were refined anisotropically and hydrogens were fixed using a riding model. CCDC1821788 and CCDC1821794 contains the supplementary crystallographic data for Complexes **1** and **2** respectively for this paper.

Density Functional Theory and Time-dependent Density Functional Theory

The density functional molecular electronic structure calculations were performed using the Gaussian09 (G09) program package[7]. The geometries of the complexes **1** and **2** were optimized in the gas phase using the B3LYP[8, 9] functional and mixed basis set for all the calculations; for Iridium the Stuttgart/Dresden (SDD) energy-consistent pseudopotentials basis set[10, 11], was used while for hydrogen, carbon, and nitrogen the 6-31G* basis set was used[12]. These ground state geometries of complexes 1 and 2 were further optimized in dichloromethane as solvent using a conductive polarizable continuum model[13, 14]. The local minima on the potential energy surface were confirmed from the positive value of the lowest vibrational frequency. Frontier molecular orbitals were visualized using Gauss view 6[15]. The orbital contribution[16] on the molecular fragments, viz. metal center and individual ligands, was analyzed by Hirshfeld's method using specialized atomic densities in the free state as implemented in the Multiwfn program[17]. The TDDFT calculation also performed on 100 states using the same level of theory and basis set in dichloromethane as solvent. The resultant UV-vis spectra are plotted using the Gabedit programme[18].

DNA Binding Studies

DNA binding studies were carried out as per our earlier report [19]. In short, absorption titration experiments were carried out using pH 7.2 phosphate buffer (containing 5% dimethylformamide) by adding the increasing concentration of CT-DNA (0–70 μM) to an iridium complex solution (10 μM). The spectra were recorded after incubation of 15 min of mixing the DNA and complex solutions. The data obtained were then fit equation 2 [20] to obtain intrinsic binding constant K_b.

$$[DNA]/[\varepsilon_a-\varepsilon_f] = [DNA]/[\varepsilon_b-\varepsilon_f] + 1/K_b\,[\varepsilon_b-\varepsilon_f] \text{ ----------(2)}$$

Where, [DNA] is the concentration of DNA in base pairs, ε_a is the extinction coefficient observed for the MLCT absorption band at the given DNA concentration, ε_f is the extinction coefficient of the complex free in solution and ε_b is the extinction coefficient of the complex

when fully bound to DNA. A plot of [DNA]/[ε_a–ε_f] versus [DNA] gave a slope 1/[ε_a–ε_f] and Y-intercept equal to 1/K_b [ε_b–ε_f], respectively. The intrinsic binding constant K_b is the ratio of the slope to the intercept [20].

Emission titration experiments were carried out using pH 7.2 phosphate buffer (containing 5% dimethylformamide) by adding the increasing concentration of DNA to metal complex solution in the buffer.

Cytotoxicity: Cell viability assay

Cytotoxicity of iridium complexes 1 and 2 against the HeLa cell line was estimated as per our earlier report[19]. The number of viable cells after appropriate treatment was determined by 3-(4,5-dimethylthiazol-2-yl)- 2,5-diphenyltetrazolium bromide (MTT; Sigma Chemical Co.) assay [21].

Fluorescence microscopic images

Hela Cells were developed on sterile glass coverslips in a 35 mm tissue culture dish and incubated at 37º under a 5% CO_2 atmosphere for 48 h. Then the culture medium was replaced with medium containing iridium complexes (10 μM). After incubation for 1 h, the medium was removed, and the cell layer was washed gently with PBS (2 mL x 3 times). Then the coverslips were mounted onto slides for measurements. Imaging was collected using high-resolution optical microscope Axio Imager M2, Carl Zeiss, Germany.

Possible types of DNA interactions

The small molecules can bind to DNA in a variety non-covalent binding modes. The three most important non-covalent DNA binding modes are: (i) electrostatic interactions, (ii) groove binding and (iii) intercalation. Electrostatic mode of DNA interactions occurs between cationic metal ions/complexes or organic molecules, and the polyanionic phosphate backbone of DNA, whereas groove binding involves direct interactions between atoms or functional groups present in a metal complex or organic molecule and those present on the edge of the base pairs in either the major or minor groove of DNA depending on size of the molecule. Intercalation is a common mode of non-covalent binding for small molecules that have polycyclic planar aromatic or heterocyclic ring systems, often in addition to a formal positive charge. These properties allow intercalator to insert and stack in between base pairs in the hydrophobic interior of helical double stranded DNA. Many molecules interact with DNA using a combination of the above binding modes that is dependent upon the specific structural characteristics of the compound under investigation.

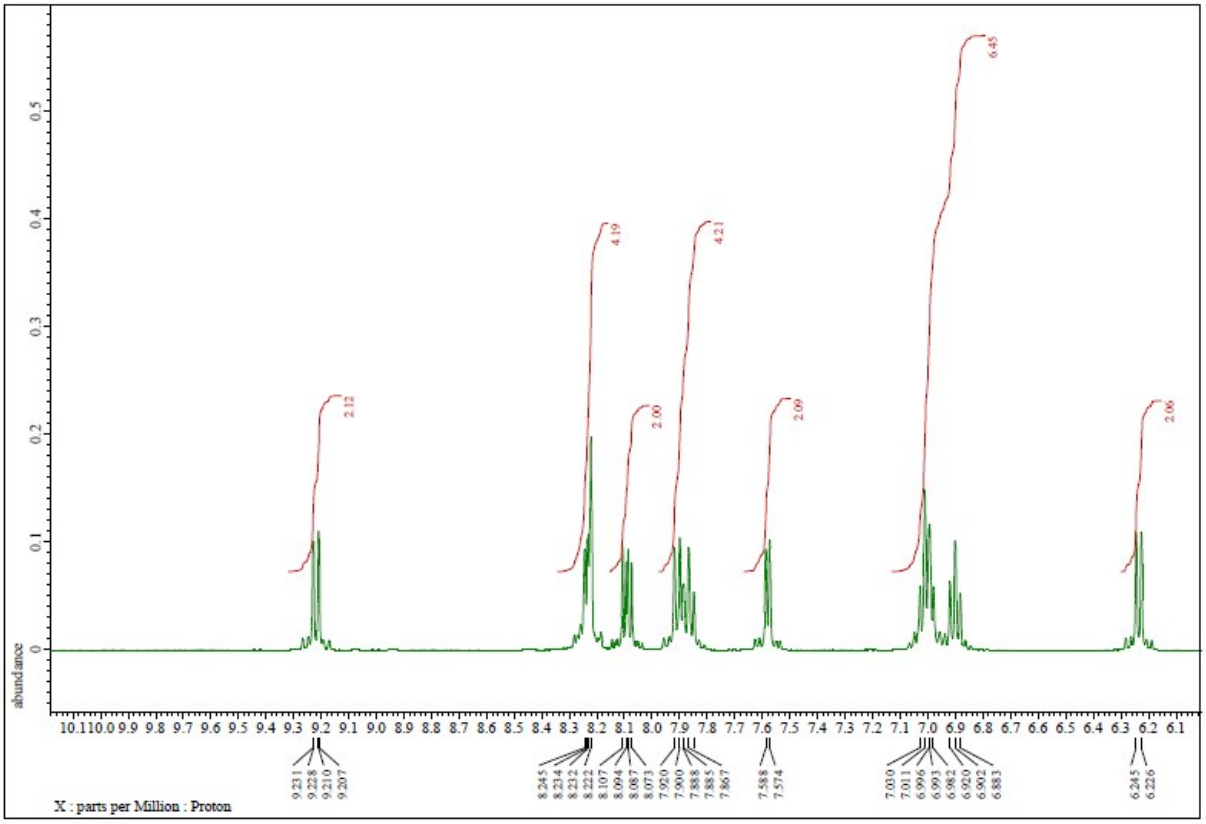

Fig. S1 ^{1}H NMR spectrum of complex 1.

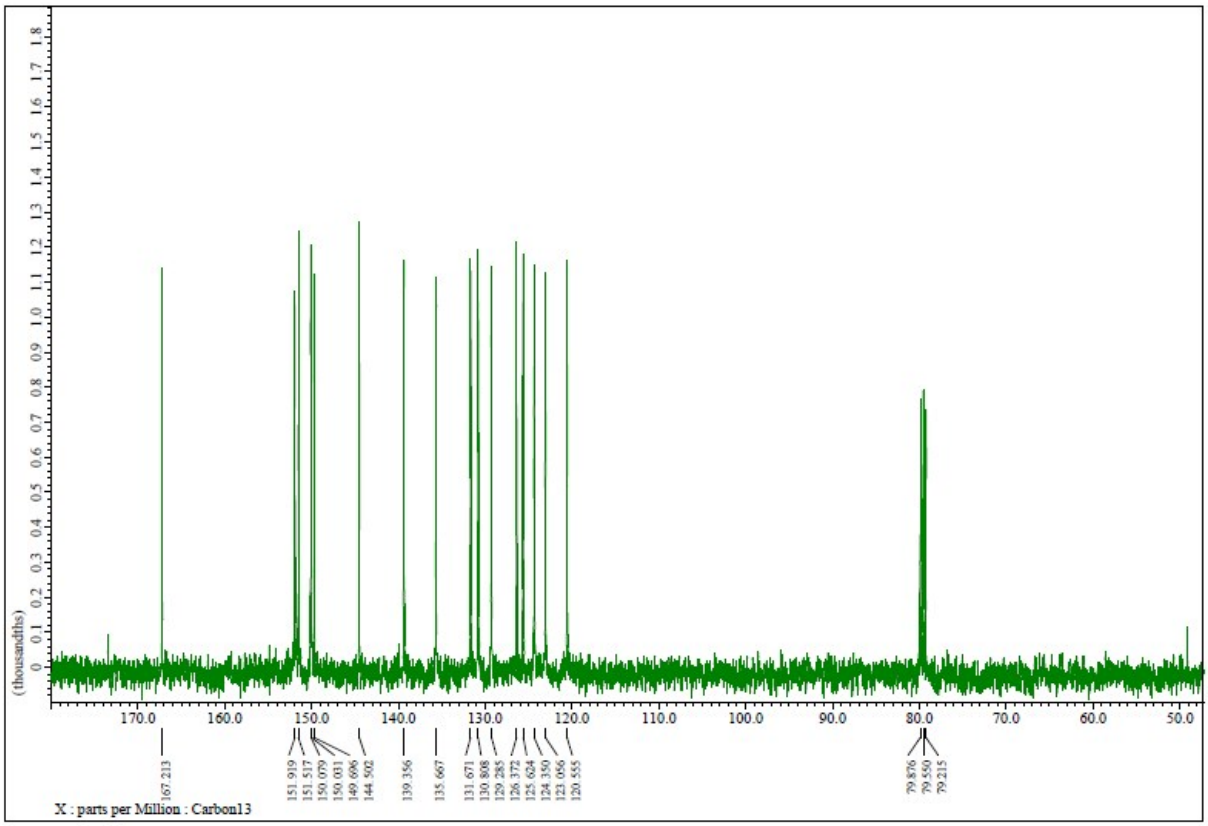

Fig. S2 ^{13}C NMR spectrum of complex 1.

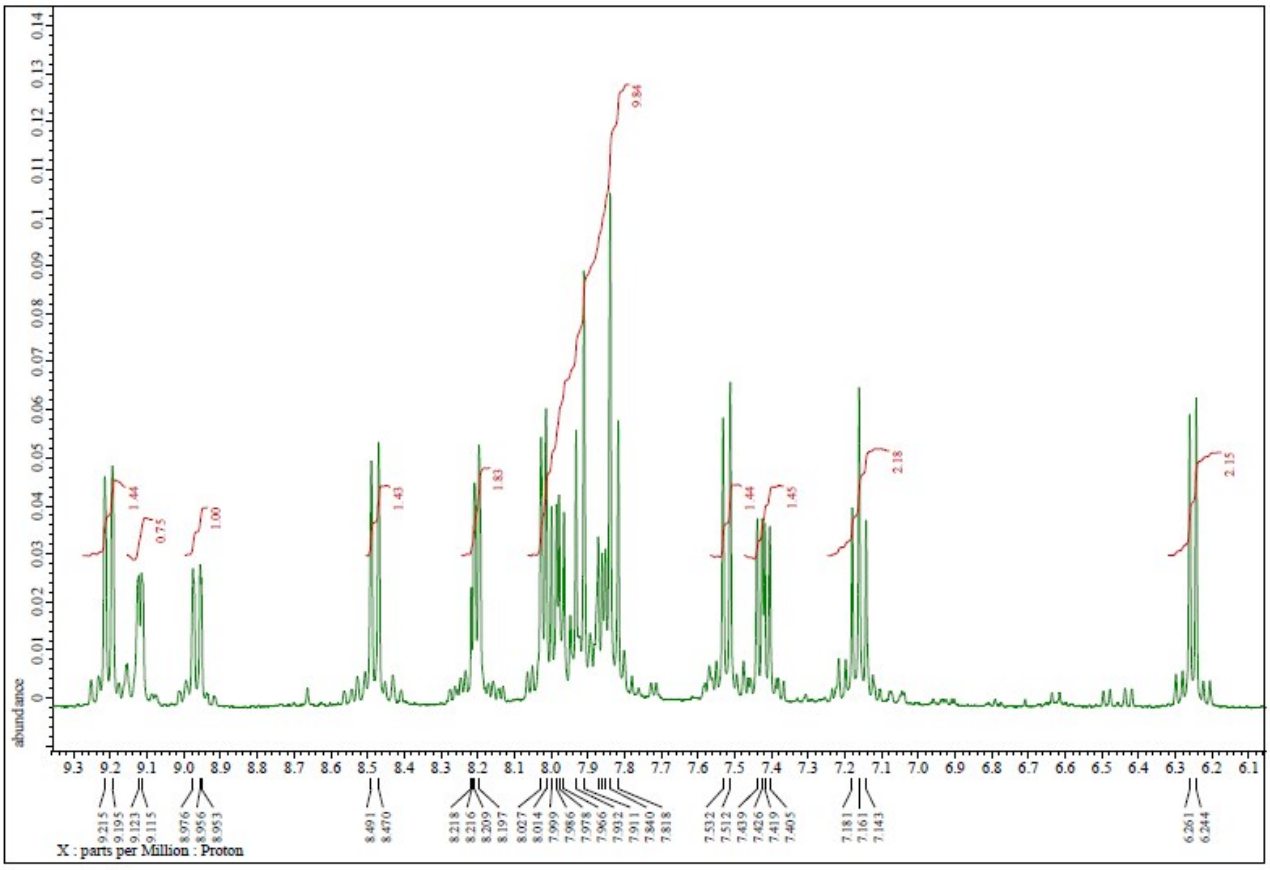

Fig. S3 ^{1}H NMR spectrum of complex 2.

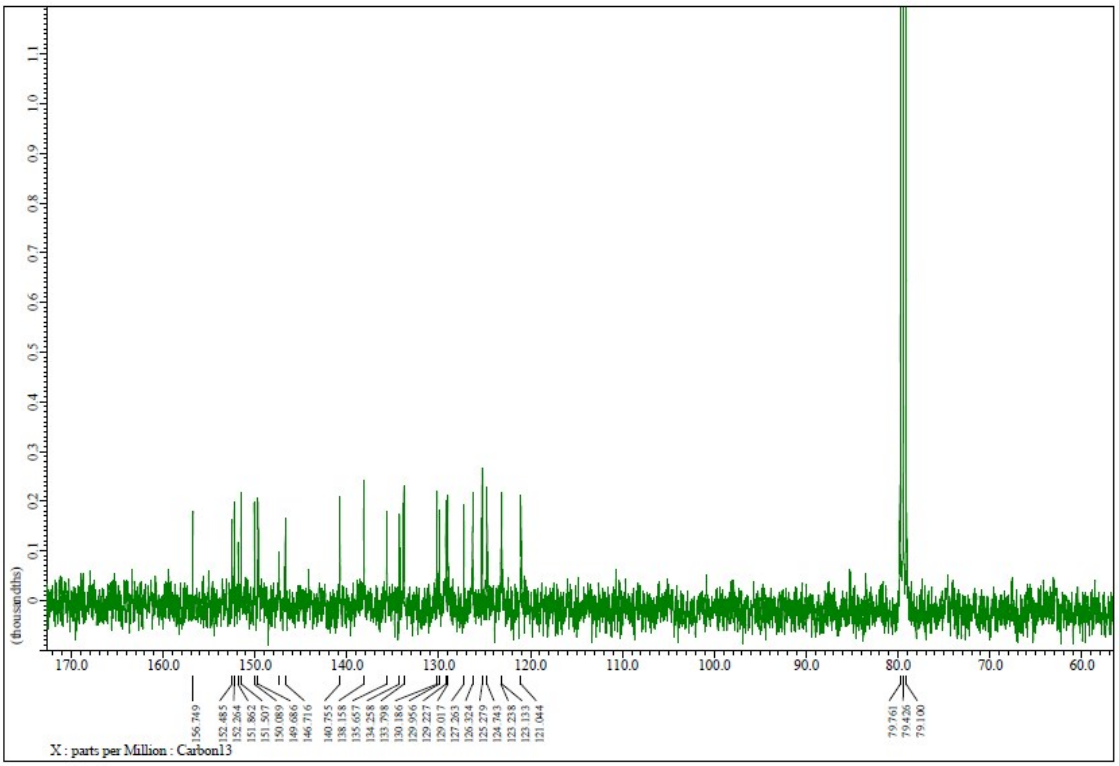

Fig. S4 ^{13}C NMR spectrum of complex 2.

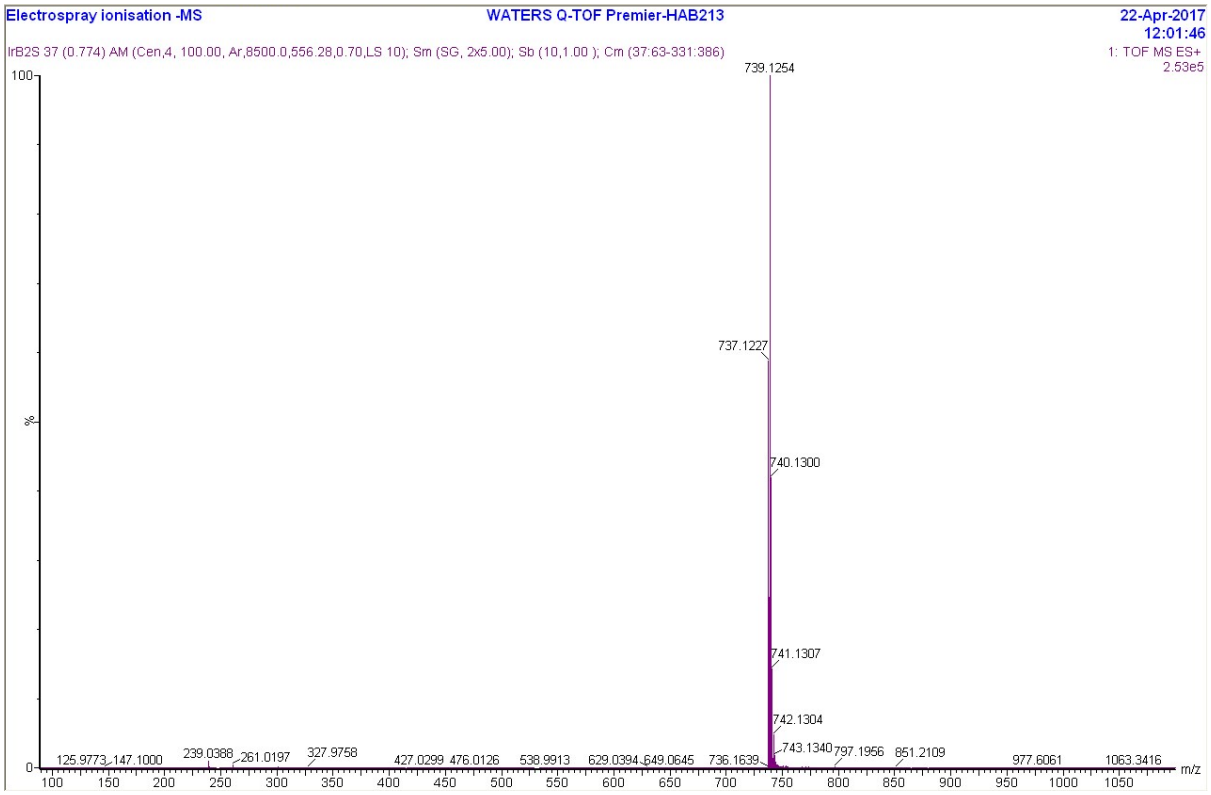

Fig S5 ESI-MS spectrum of complex 1.

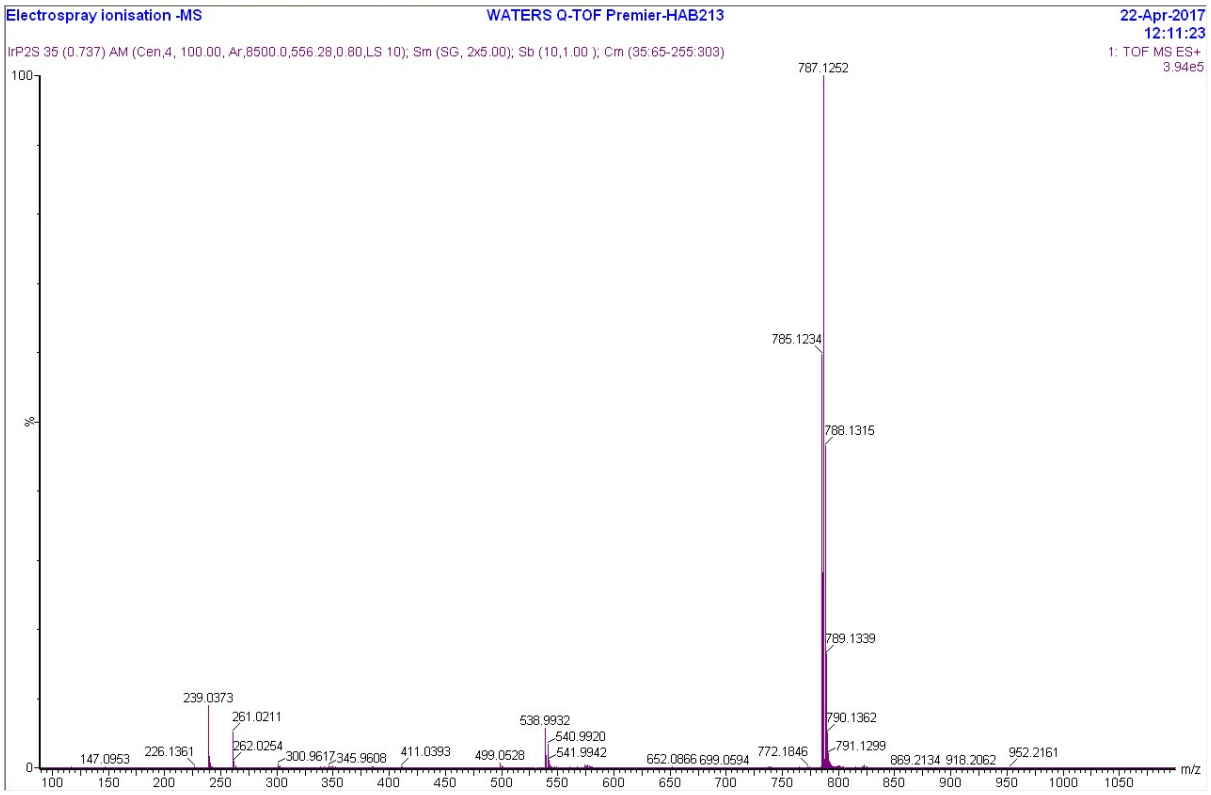

Fig. S6 ESI-MS spectrum of complex **2**.

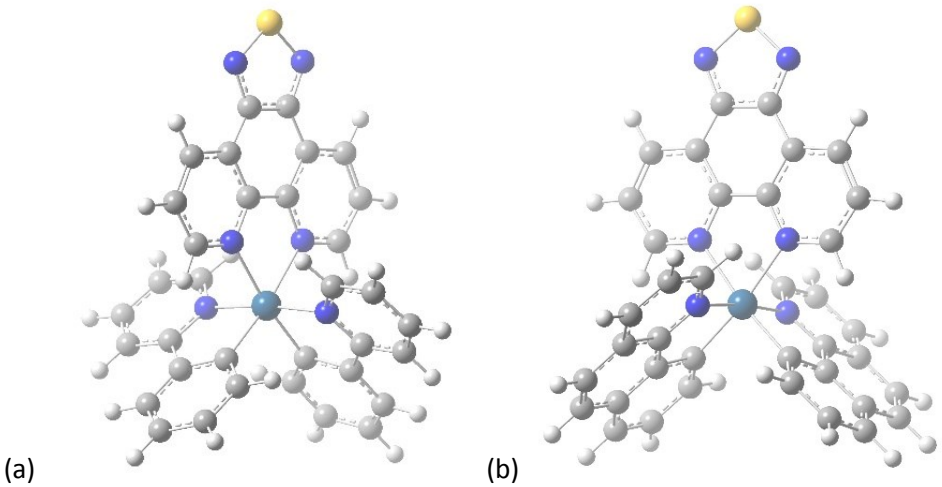

Fig. S7 The B3LYp optimized geometries of complexes (a) **1** and (b) **2**.

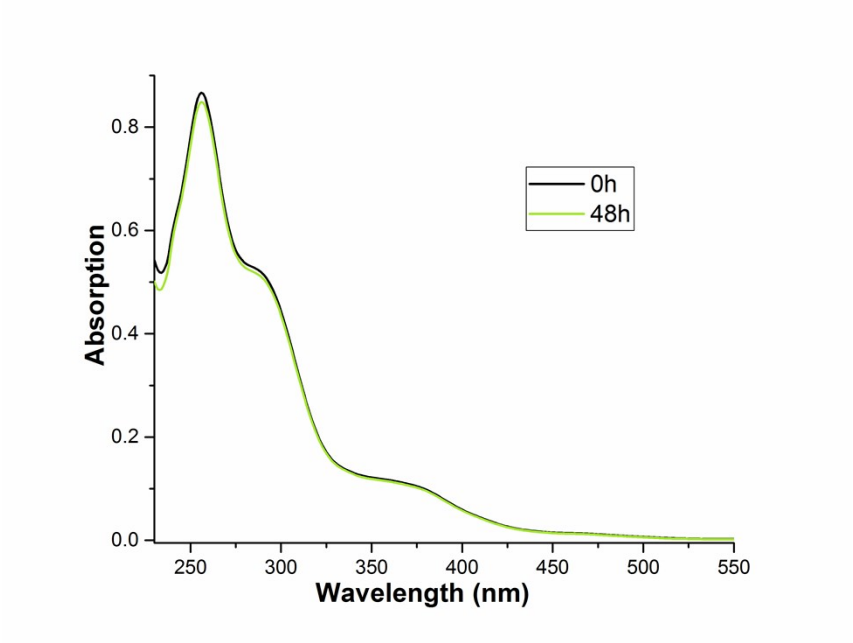

Fig. S8 UV-Vis spectra of complex **1** in water immediately after dissolving and after 48h of dissolving the complex in water.

Table S1. The frontier molecular orbitals for the DFT optimized geometry of the complexes **1** and **2**.

Ir2bs	**Irpt2**
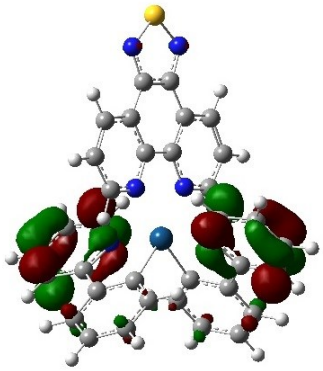 LUMO+5 (-0.05257 au)	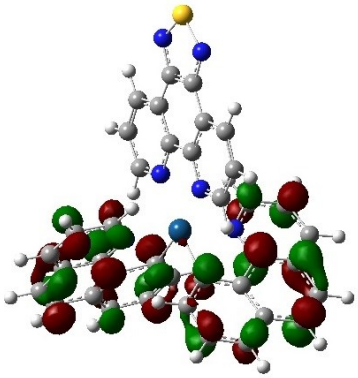 LUMO+5 (-0.05510 au)
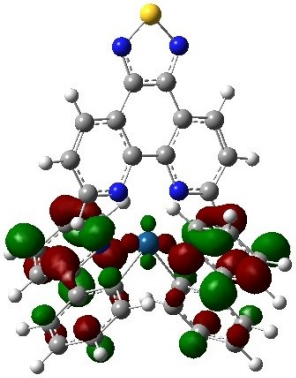 LUMO+4 (-0.06949 au)	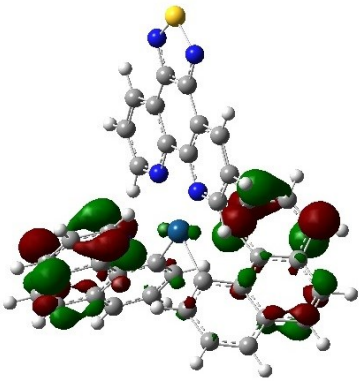 LUMO+4 (-0.07826 au)
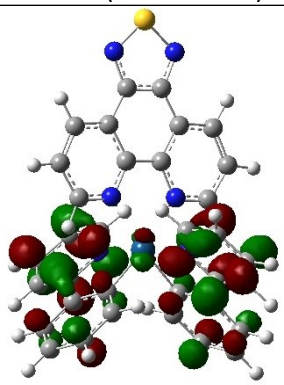 LUMO+3 (-0.07253 au)	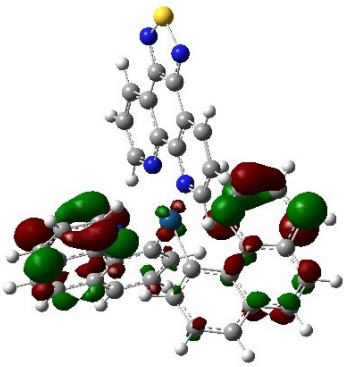 LUMO+3 (-0.07882 au)
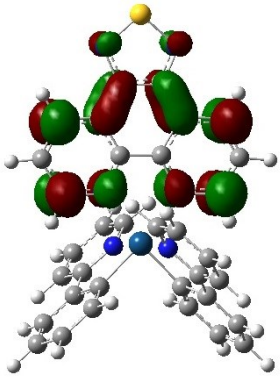 LUMO+2 (-0.08519 au)	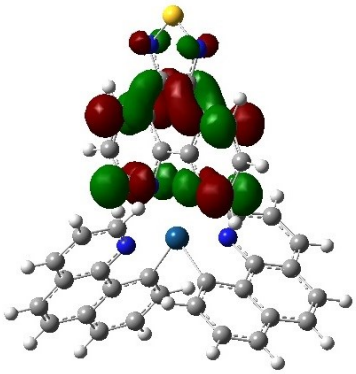 LUMO+2 (-0.08535 au)

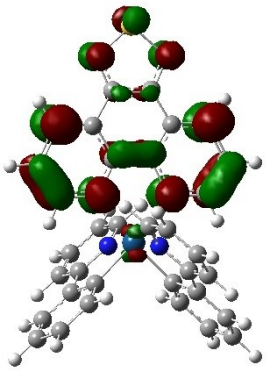 LUMO+1 (-0.09968 au)	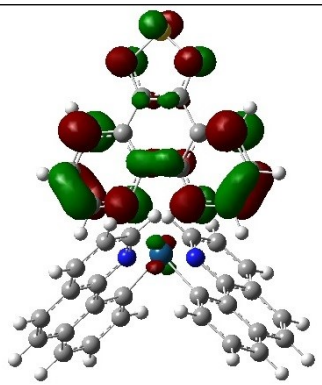 LUMO+1 (-0.09973 au)
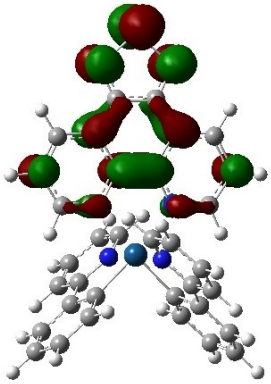 151 LUMO (-0.11088 au)	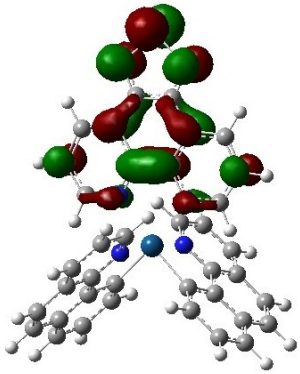 163 LUMO (-0.11082 au)
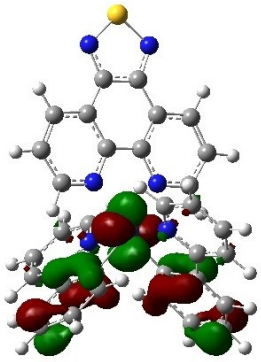 150 HOMO (-0.21599 au)	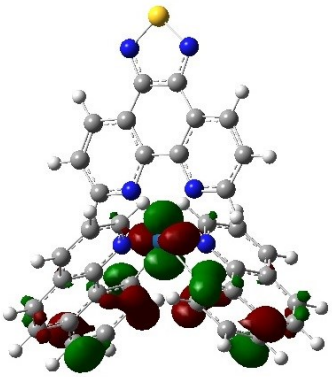 162 HOMO (-0.21302 au)
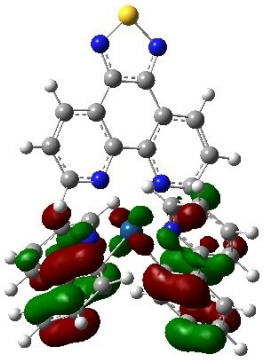 HOMO-1 (-0.23878 au)	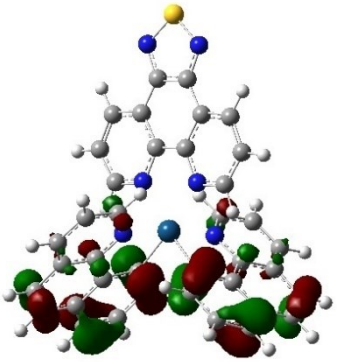 HOMO-1 (-0.22984 au)

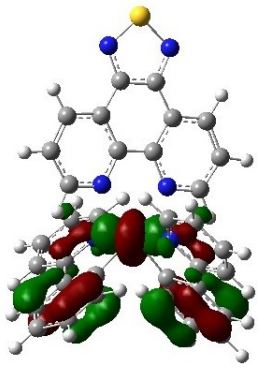 HOMO-2 (-0.24488 au)	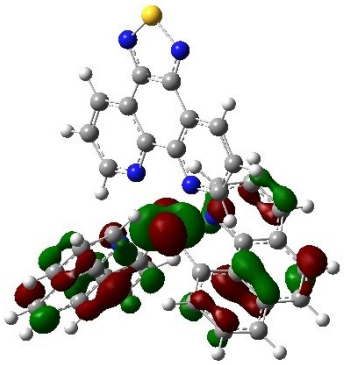 HOMO-2 (-0.24143 au)
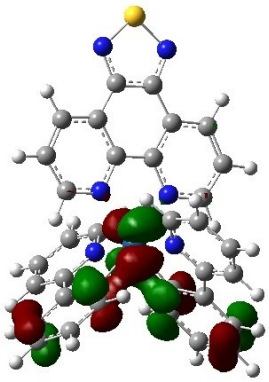 HOMO-3 (-0.24874 au)	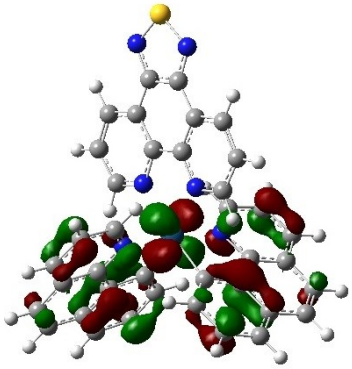 HOMO-3 (-0.24464 au)
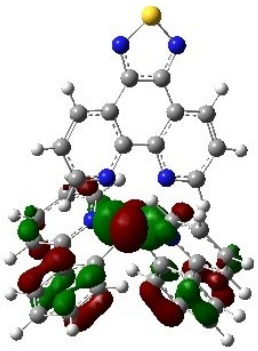 HOMO-4 (-0.25174 au)	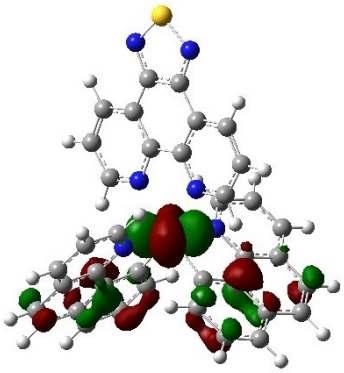 HOMO-4 (-0.25708 au)
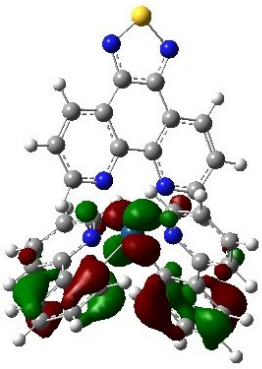 HOMO-5(-0.25496 au)	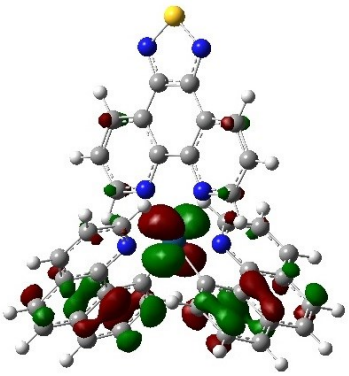 HOMO-5 (-0.25928 au)

Table S2: Orbital contribution of frontier molecular orbitals.

Orbital type	Complex 1						Complex 2					
	Orbital number	Ene(a.u.)	Composition				Orbital number	Ene(a.u.)	Composition			
			Ru	L1	L2	L2'			Ru	L1	L3	L3'
HOMO-5	145	-0.2550	23.7	6.9	34.7	34.7	157	-0.2593	34.9	12.8	26.2	26.2
HOMO-4	146	-0.2517	39.6	4.5	28.0	27.9	158	-0.2571	43.7	6.0	25.2	25.2
HOMO-3	147	-0.2487	34.9	9.1	28.0	28.1	159	-0.2446	26.8	5.4	33.9	33.9
HOMO-2	148	-0.2449	30.3	3.0	33.4	33.3	160	-0.2414	27.8	2.4	34.9	34.9
HOMO-1	149	-0.2388	6.2	1.6	46.1	46.1	161	-0.2298	1.9	1.4	48.4	48.4
HOMO	150	-0.2160	35.2	3.1	30.9	30.8	162	-0.2130	26.7	2.6	35.3	35.3
LUMO	151	-0.1109	0.7	98.6	0.4	0.4	163	-0.1108	0.7	98.7	0.3	0.3
LUMO+1	152	-0.0997	2.9	95.5	0.8	0.8	164	-0.0997	2.9	95.5	0.8	0.8
LUMO+2	153	-0.0852	1.1	97.2	0.9	0.9	165	-0.0853	1.3	94.3	2.2	2.2
LUMO+3	154	-0.0725	4.2	1.7	47.0	47.0	166	-0.0788	3.1	1.1	47.9	47.8
LUMO+4	155	-0.0695	4.3	2.3	46.6	46.7	167	-0.0783	2.3	4.8	46.4	46.5
LUMO+5	156	-0.0526	1.4	5.9	46.3	46.4	168	-0.0551	2.1	2.4	47.8	47.7

Table S3: Details of the transitions UV-visible spectra of complexes calculated using TD-DFT.

Sr. No.	State	Energy in eV (nm)	Oscillator strength	Transition (contribution)
Complex 1				
1.	S1 (ES2)	2.3082 (537.14)	0.0002	HOMO ->LUMO 0.6439 HOMO ->LUMO+1 0.28688
2.	S2 (ES4)	2.5809 (480.39)	0.0004	HOMO ->LUMO -0.28861 HOMO ->LUMO+1 0.64158
3.	S3 (ES9)	2.9527 (419.91)	0.0003	HOMO ->LUMO+2 0.70070
4.	S4 (ES11)	3.0183 (410.77)	0.0190	HOMO-3 ->LUMO 0.13687 HOMO-1 ->LUMO 0.66193 HOMO-1 ->LUMO+1 0.17347
5.	S5 (ES13)	3.0503 (406.47)	0.0001	HOMO-4 ->LUMO 0.30029 HOMO-4 ->LUMO+1 0.18105 HOMO-2 ->LUMO 0.54946 HOMO-2 ->LUMO+1 0.27031
6.	S6 (ES16)	3.1525 (393.28)	0.0628	HOMO ->LUMO+3 0.69707
7.	S7 (ES17)	3.1963 (387.90)	0.0658	HOMO-5 ->LUMO 0.21520 HOMO-3 ->LUMO 0.59749 HOMO-3 ->LUMO+1 0.17934 HOMO-1 ->LUMO -0.16875 HOMO ->LUMO+4 -0.16012
Complex 2				
1.	S1 (ES2)	2.2646 (547.48)	0.0002	HOMO ->LUMO 0.65286 HOMO ->LUMO+1 0.26163
2.	S2 (ES4)	2.5313 (489.80)	0.0000	HOMO ->LUMO -0.26539 HOMO ->LUMO+1 0.65023
3.	S3 (ES10)	2.8231 (439.18)	0.0043	HOMO-1 ->LUMO 0.68743 HOMO-1 ->LUMO+1 0.16175
4.	S4 (ES12)	2.8954 (428.22)	0.0000	HOMO-1 ->LUMO+1 0.10886 HOMO ->LUMO+2 0.68789
5.	S5 (ES15)	2.9958 (413.87)	0.0261	HOMO-4 ->LUMO 0.13328 HOMO-2 ->LUMO 0.45040 HOMO-2 ->LUMO+1 0.19085 HOMO ->LUMO+3 0.47138
6.	S6 (ES16)	3.0050 (412.59)	0.0323	HOMO-4 ->LUMO -0.12921 HOMO-2 ->LUMO -0.41792 HOMO-2 ->LUMO+1 -0.18438 HOMO ->LUMO+3 0.50650
7.	S7 (ES19)	3.0401 (407.83)	0.0024	HOMO-1 ->LUMO+1 -0.18022 HOMO ->LUMO+4 0.66017
8.	S8 (ES20)	3.0918 (401.01)	0.0000	HOMO-1 ->LUMO -0.15123 HOMO-1 ->LUMO+1 0.65302 HOMO ->LUMO+2 -0.12932 HOMO ->LUMO+4 0.16293
9.	S9 (ES22)	3.1158 (397.92)	0.0747	HOMO-5 ->LUMO 0.16228 HOMO-3 ->LUMO 0.64672 HOMO-3 ->LUMO+1 0.17383 HOMO ->LUMO+4 0.11716

References:

1. J. R. Lakowicz, *Principles of Fluorescence Spectroscopy*, Springer US, 3 edn., 2006.
2. A. Juris, V. Balzani, F. Barigelletti, S. Campagna, P. Belser and A. von Zelewsky, *Coordination Chemistry Reviews*, 1988, **84**, 85-277.
3. J. V. Caspar and T. J. Meyer, *Journal of the American Chemical Society*, 1983, **105**, 5583-5590.
4. Bruker, *Journal*, 2010.
5. O. V. Dolomanov, L. J. Bourhis, R. J. Gildea, J. A. K. Howard and H. Puschmann, *Journal of Applied Crystallography*, 2009, **42**, 339-341.
6. G. Sheldrick, *Acta Crystallographica Section A*, 2008, **64**, 112-122.
7. M. J. Frisch, G. W. Trucks, H. B. Schlegel, G. E. Scuseria, M. A. Robb, J. R. Cheeseman, G. Scalmani, V. Barone, G. A. Petersson, H. Nakatsuji, X. Li, M. Caricato, A. V. Marenich, J. Bloino, B. G. Janesko, R. Gomperts, B. Mennucci, H. P. Hratchian, J. V. Ortiz, A. F. Izmaylov, J. L. Sonnenberg, Williams, F. Ding, F. Lipparini, F. Egidi, J. Goings, B. Peng, A. Petrone, T. Henderson, D. Ranasinghe, V. G. Zakrzewski, J. Gao, N. Rega, G. Zheng, W. Liang, M. Hada, M. Ehara, K. Toyota, R. Fukuda, J. Hasegawa, M. Ishida, T. Nakajima, Y. Honda, O. Kitao, H. Nakai, T. Vreven, K. Throssell, J. A. Montgomery Jr., J. E. Peralta, F. Ogliaro, M. J. Bearpark, J. J. Heyd, E. N. Brothers, K. N. Kudin, V. N. Staroverov, T. A. Keith, R. Kobayashi, J. Normand, K. Raghavachari, A. P. Rendell, J. C. Burant, S. S. Iyengar, J. Tomasi, M. Cossi, J. M. Millam, M. Klene, C. Adamo, R. Cammi, J. W. Ochterski, R. L. Martin, K. Morokuma, O. Farkas, J. B. Foresman and D. J. Fox, *Journal*, 2016.
8. A. D. Becke, *Physical Review A*, 1988, **38**, 3098-3100.
9. A. D. Becke, *The Journal of Chemical Physics*, 1993, **98**, 5648-5652.
10. M. Dolg, H. Stoll and H. Preuss, *Theoretica chimica acta*, 1993, **85**, 441-450.
11. M. D. U. Wedig, H. Stoll, *Quantum Chemistry: The Challenge of Transition Metals and Coordination Chemistry*, Springer Netherlands, 1986.
12. K. B. Wiberg, *Journal of Computational Chemistry*, 1986, **7**, 379-379.
13. S. Fantacci, F. De Angelis and A. Selloni, *Journal of the American Chemical Society*, 2003, **125**, 4381-4387.
14. S. Fantacci, F. De Angelis, A. Sgamellotti and N. Re, *Chemical Physics Letters*, 2004, **396**, 43-48.
15. S. M. Semichem Inc., KS, 2016, *Journal*, 2016.
16. C. F.-W. LU Tian, *Acta Chimica Sinica*, 2011, **69**, 2393-2406.
17. T. Lu and F. Chen, *Journal of Computational Chemistry*, 2012, **33**, 580-592.
18. A.-R. Allouche, *Journal of Computational Chemistry*, 2011, **32**, 174-182.
19. S. S. Bhat, V. K. Revankar, R. V. Pinjari, N. S, C. Bogar, K. Bhat and V. A. Kawade, *New Journal of Chemistry*, 2017, **41**, 5513-5520.
20. A. Wolfe, G. H. Shimer and T. Meehan, *Biochemistry*, 1987, **26**, 6392-6396.
21. J. S. Chen, M. Konopleva, M. Andreeff, A. S. Multani, S. Pathak and K. Mehta, *J Cell Physiol*, 2004, **200**, 223-234.